IOP Conf. Series: Materials Science and Engineering **299** (2018) 012083 doi:10.1088/1757-899X/299/1/012083

Synthesis of Zeolite-X from Bottom Ash for H_2 Adsorption

R Y Kurniawan[1], T Q Romadiansyah[1], A D Tsamarah[1], and N Widiastuti[1*]

[1]Chemistry Department, Faculty of Science, Institut Teknologi Sepuluh Nopember (ITS), Jl. Arief Rahman Hakim, 60111, Surabaya.

Email : nurul_widiastuti@chem.its.ac.id

Abstract. Zeolite-X was synthesized from bottom ash power plant waste using fusion method on air atmosphere. The fused product dissolved in demineralized water and aluminate solution was added to adjust the SiO_2/Al_2O_3 molar ratio gel prior hydrothermal process. The synthesis results were characterized using X-Ray Diffraction (XRD), Scanning Electron Microscope (SEM), and Fourier Transform Infrared (FTIR). The results showed that the zeolite-X has a high crystallinity with octahedral particle. The pure-form zeolite-X then was characterized and tested for H_2 gas adsorption by gravimetric method to determine the H_2 gas adsorption capacity of zeolite-X from bottom ash and it was compared to synthetic zeolite-X.

1. Introduction

Hydrogen is potentially ideal energy sources for fossil fuel replacement. The reasons for this is due to highly reactive, bumpy gas, relatively small size, thus resulting in easily stored in a particular material and promosing to be applied in fuel cell vehicle. It also occurs at high level of energy, which reaches up to 142 MJ/kg [1]. Besides, hydrogen is environmentally friendly energy source, clean and only produce water residue as a result of hydrogen combustion with O_2 gas in fuel cell. Therefore, hydrogen technology has been developed in various developed countries such as such as United State of America, Republic of South Korea and Japan [2-3]. Nevertheless, the development of hydrogen technology as an alternative energy source requires a variety of considerations. One of the challenges in the development of hydrogen technology is finding materials with large amounts of hydrogen storage up to 6-9 wt% in accordance with the targets proposed by the Department of Energy (DoE) in USA in 2010-2015 [4].

Porous materials has been the subject of research in developing hydrogen storage such as zeolites, carbon nanotubes, nano fibers, metal organic frameworks and other porous materials. Among the materials, zeolite-X, a porous alumina-silicate material is often highlighted to be a hydrogen storage material owing to having pore diameter size of 3-8 Å [7, 8]. With this pore size, hydrogen gas with the size of 2.890 Å can be well absorbed into the zeolite-X pores [9]. This material meets with the requirement of hydrogen storage material, that has high porosity, high surface area, diameter pore size equal or greater than the size of the gas molecule [6].

However, zeolite-X is generally synthesized from synthetic materials, which has disadvantages, such as a high cost for synthesis and waste production. Therefore, it is necessary to look for another way of synthesizing zeolites from the lowest cost material. Research on the synthesis of zeolites that

has been developed recently is utilizing fly ash as the precursor. Various types of synthesized zeolites from fly ash are zeolite-X and zeolite-A [10-11]. Another study also reported that zeolite-X with high crystallinity can be synthesized from fly ash by fusion method followed by hydrothermal treatment [12].

Fly ash is a hazardous waste derived from power plants, which is a non-carbonaceous and has mild mass fraction. Instead of fly ash, other types of waste derived from power plant is bottom ash, which is also classified as a hazardous waste [13]. Unlike fly ash, bottom ash has a heavier mass fraction because it still contains carbon residues as well as impurities such as metal oxides. This condition makes the utilization of bottom ash lower compared to fly ash.

The chemical components contained in the bottom ash are silicon (Si) 24.10%, aluminum (Al) 6.80%, iron (Fe) 33.59%, calcium (Ca) 26.30% and carbon (C) is around 11.2% of the total weight [14]. The proportion of the chemical content of the bottom ash shows that the bottom ash has the same content as the fly ash. Hence, the bottom ash can be used as an alternative material for zeolites especially for zeolite-X.

The synthesis of zeolite-X from the bottom ash are also performed through a fusion process using alkali followed by a hydrothermal process like the synthesis of zeolite-X from fly ash. In the previous research, zeolite-X with high crystallinity can be synthesized at temperature of 100°C for 15 hours and its crystallinity decrease as the hydrothermal time increases [15]. Therefore, in the present study, the zeolite-X was synthesized from the bottom ash at the temperature of 100°C for 15 hours to produce a high crystallinity of zeolite for hydrogen adsorption.

2. Materials and methods

2.1. Equipments and Materials

The equipments used were hydrothermal reactor (stainless steel autoclave), gravimetry equipment. The materials used were bottom ash from power plant, solid $NaAlO_2$ (Sigma Aldrich), Na_2SiO_3 solution (Sigma Aldrich), NaOH pellet (99% p.a) (Sigma Aldrich), HCl 37% (SAP) and H_2 Ultra High Purity (UHP) gas. Characterization was performed using X-Ray Diffraction (XRD) Expert Pan Analytical, Scanning Electron Microscope (SEM) SU 3500 and Fourier Transform Infrared (FTIR) Thermo Scientific Nicolet iS10.

2.2. Procedures

2.2.1. Preparation of Bottom Ash. The bottom ash was first sieved with a size of 60 mesh sieve to obtain fine and uniform particles. This fine bottom ash was then heated at 110°C for 3 hours. Meanwhile, to reduce the excess of Fe and Ca contents in the bottom ash, Fe and Ca separations were performed using ferrite magnet and HCl 37%.

2.2.2. Extraction of Si and Al from Bottom Ash. In this study, zeolite-X was synthesized using a fusion method, followed by hydrothermal treatment. The bottom ash melting process was carried out by mixing the bottom ash with alkali (NaOH) with a proportional ratio of the bottom ash: NaOH =1:1, then heated in a blast tube at 750°C in the air atmosphere. The solids obtained from the melting process were then weighed and dissolved in 12 mL/g of demineralized water. The solution was stirred and aged in a polyethylene bottle for 2 hours at room temperature. The solution was filtered to separate the residue from the solution. The filtrate obtained from the filtration process was the source of Na, Si and Al as a precursor for synthesizing zeolite. *2.2.3. Synthesis of Zeolite-X.* Zeolite-X was synthesized from the extract solution obtained from the melting process by adjusting the molar composition to reach $NaAlO_2$: 4 SiO_2: 16 NaOH: 325 H_2O [16] by adding $NaAlO_2$-NaOH solution. The zeolite-X mixture or slurry was put into a sealed hydrothermal reactor for the crystallization process of zeolite-X. The hydrothermal process of zeolite-X was carried out at temperature of 100°C

for 15 hours. The solid obtained from the hydrothermal crystallization was separated from the filtrate, then washed with distilled water until pH 9-10 and dried in an oven at 105°C for 24 hours.

2.2.4. Characterization. The solids obtained from the synthesis process were characterized by X-Ray Diffraction (XRD) to determine the crystallinity of the zeolite formed. The structural morphology of the zeolite-X is observed by Scanning Electron Microscopy (SEM) and the fungsional groups of the zeolite-X after adsorption was observed by Fourier Transform Infrared (FTIR).

2.2.5. H_2 gas Adsorption. Determination of H_2 gas adsorption capacity on the bottom ash based zeolite-X was performed using gravimetric method as presented in Fig.1. Firstly, the sample of zeolit-X was degassed at 350°C under vacuum condition. Gravimetric method was performed at 30°C. The hydrogen gas was fed into the cell sample through the zeolite-X sample and the gas flow was set constant at a rate of 20 ml/min. Data are taken every one minute until a constant weight was obtained. The weight was recorded as the final weight after the adsorption process (m_t)

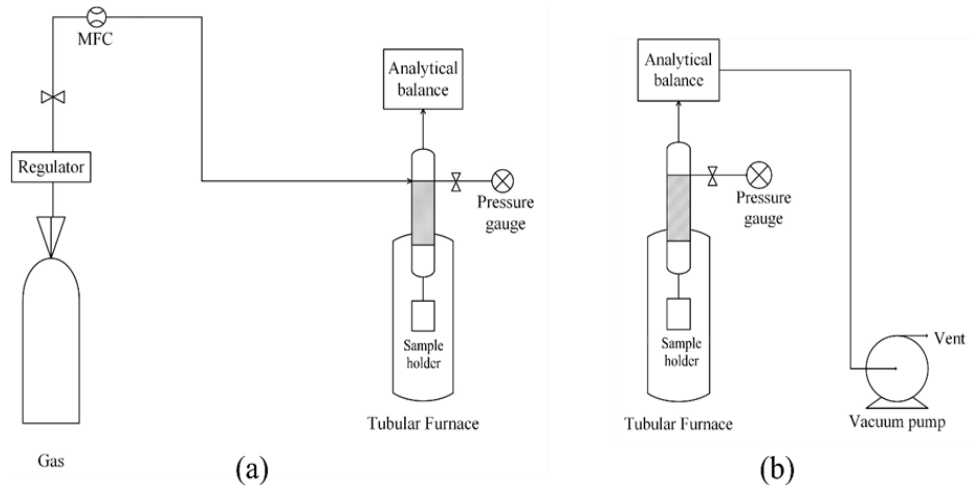

Fig.1 – Schematic diagrams of (a) adsorption and (b) desorption

3. Results and discussions

3.1. Preparation of Si and Al from Bottom Ash

This research was started by the determination of chemical composition of the bottom ash using X-Ray Flourescence Instrument (XRF). The determination of chemical composition contained in the bottom ash was very important to obtain the percentage of Si and Al weight content in the bottom ash as a precursor in the synthesis of zeolite. The result of bottom ash analysis with X-Ray Flourescence (XRF) can be seen in Table 1.

Table 1. Result of bottom ash chemical composition analysis.

Sample	Component (%)			
	Si	**Al**	**Fe**	**Ca**
Bottom Ash Before Separation	15.2	5.5	48.4	25.5
Bottom Ash After Separation	37.1	3.8	21.5	9.1

Table 1 shows that bottom ash contains a high percentage of Si and Al in their oxide forms, they are 15.2% and 5.5%. Due to the presence of Si and Al content, the bottom ash has the potential to be utilized as a precursor in the synthesis of zeolites. The value of Si and Al content was used in

determining the Si/Al ratio in the synthesis of zeolite. The ratio value affected the type of zeolite formed. The low ratio of Si/Al is suitable for zeolite synthesis with low Si values such as Zeolite-X. Beside Si and Al, the bottom ash also contains a high percentage of Fe and Ca. Previous research also presented the same result that Fe and Ca were the main content of bottom ash beside Si and Al [17]. The high content of Ca and Fe can be separated using ferrite magnet and 37% HCl. The results of the separation were then re-analyzed using X-Ray Flourescence (XRF) to determine the value of Ca and Fe content after the separation process, the result of the bottom ash after separation is shown in Table 1.

The amount of components in the bottom ash changes after the separation process. Fe content decreased by 55.57%, while Ca content decreased by 64.31%. The reduction of the composition shows that Ca in calcite phase ($CaCO_3$) and calcium oxide (CaO) have reacted with HCl to form water-soluble $CaCl_2$. The decrement of Fe and Ca content shows that the separation process using ferrite magnet and concentrated HCl decreased the Fe and Ca content from the bottom ash effectively to reduce the oxide impurity of bottom ash.

In addition to the reduction amount of Fe and Ca content, Al content also decreased because Al also reacted with the concentrated HCl to form $AlCl_3$. On the other hand, the Si content has increased after the separation because of reducing the impurity. The results is in accordance with the result of bottom ash characterization using XRD after the separation as shown in Figure 2. The mineral phase of bottom ash after separation is dominated by quartz phase (SiO_2), while the impurity phases such as hematite in the form of Fe_2O_3 and calcite in the form of $CaCO_3$ and CaO have a fairly low intensity and distribution. This is in accordance with the results of XRF characterization, which showed that Fe and Ca content decreased in bottom ash after the separation process. In addition, there was also a mullite phase containing Al. Given the Si and Al content found in the bottom ash, it allows the zeolite to be synthesized from the bottom ash.

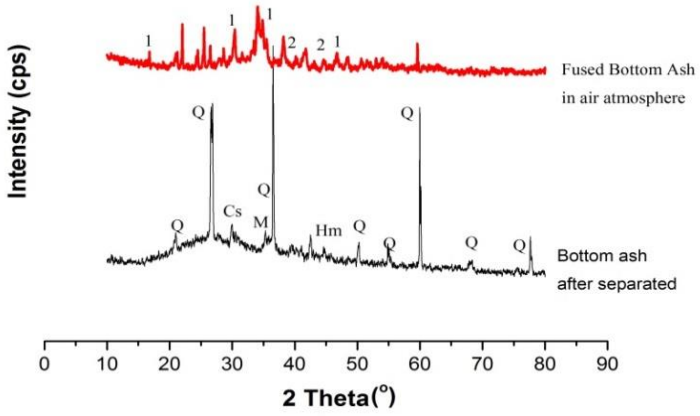

Figure 2. Difractogram of the fused bottom ash compared to the bottom ash before fused (1 = Sodium Silicate, 2 = Sodium Aluminum Silicate, Q = Quartz; M = Mullite; Hm = Hematite; Ks = Calcite).

However, quartz (SiO_2) and mullites are minerals that have small solubility values in water, thus, the bottom ash must be firstly fused in air atmosphere using alkali at high temperatures. The bottom ash-melting solids are then characterized by XRD to determine the mineral phase formed after the melting as shown in Figure 1. The difractogram shows the difference of the bottom ash before the melting process, that is the loss of peaks of hematite and calcite. In addition, the other crystalline phase peaks such as quartz and mullites are largely disappearing as well. This indicates that the quartz and mullite have reacted with the base (NaOH) and activated to produce a soluble salt in the form of sodium silicate (peak 1) (PDF 16-0818) and aluminum silicate salt (peak 2) (PDF 33-1203). This proves that the melting process at high temperatures was an effective method to extract the Si and Al content from the bottom ash into a soluble salt.

Previous researches have also reported that the fusion process of fly ash using alkali at high temperatures can change the fly ash mineral phases that are difficult to dissolve into a soluble sodium silicate and amorphous aluminum silicate [20-22]. Sodium silicate and sodium aluminum silicate were produced through the melting process, which were the major components in the formation of zeolites. After obtaining sodium silicate and sodium aluminum silicate from the fusion process, then extraction process of the solid (obtained from the fusion process) was conducted in order to obtain the dissolved Si and Al components. The extraction process in this study was conducted by mixing solids of demineralized fermentation. The obtained filtrate then tested by ICP-AES to determine the level of Si, Al and Na components contained in the filtrate, it is used for the determination of Si/Al ratio. The results of component analysis of Si, Al and Na using ICP-AES are shown in Table 2.

Table 2. The results of the fused bottom ash extract concentration analysis.

Sample	Component (ppm)		
	Si	**Al**	**Na**
Extract of fused bottom ash	3160.7	35.19	5833.3

In Table 2, it was found that the concentration of Al in the extract solution tended to be smaller than the Si and Na concentrations. This is because Al has a lower solubility value in an alkaline solution compared to Si, thus Al was more retained in the residual residue of the extract. With the low solubility value of Al in the extract, the Si / Al molar ratio value were high indicating not suitable for zeolite-X synthesis. Therefore, to adjust the Si/Al molar ratio composition according to the zeolite-X molar ratio, it was necessary to add $NaAlO_2$-NaOH solution as an external Al source. The addition of Al source aims to minimize the molar ratio of the aluminosilikat gel.

3.2. Synthesis of Zeolite-X from Bottom Ash

The bottom ash smelting extract with alkali was then used as the precursor in the synthesis of zeolite-X. The extracts are arranged in the composition of the molar ratio corresponding to the Na-Zeolite-X NaO: 4 SiO_2: 16 NaOH: 325 H_2O with the addition of $NaAlO_2$-NaOH solution to obtain mixed or slurry solution. The result of hydrothermal process was white solid and colorless filtrate. The solid formed has a pH of 14 indicating that the zeolite-X was formed because the zeolite-forming anion, $Si(OH)^{4-}$ at pH> 12 [23].

3.3. Characterization of Zeolite-X from Bottom Ash

The XRD characterization of the zeolite-X has a typical zeolite-X peak at 2θ = 6.25 °; 10,35 °; 15.80 °; 20.43 °; 23.62 °; 23.73 °; 27.05 ° and 31.30 °as shown in Figure 3. In addition, the pattern of the synthesized zeolite diffractogram also has the same pattern as the peak standard (the X mark). This indicates that the bottom ash based zeolite-X has been successfully synthesized.

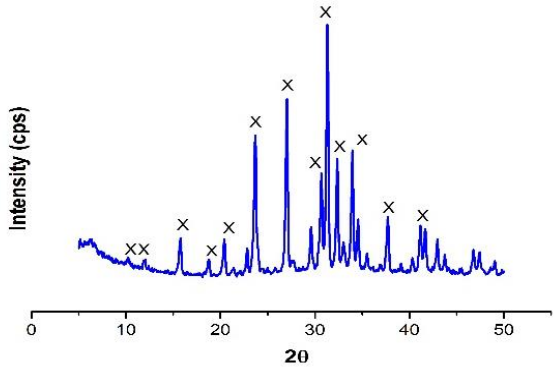

Figure 3. Difractogram of zeolite-X from bottom ash

The high level of crystallinity of the zeolite-X is also supported by the Zeolite-X morphology from the SEM characterization as shown in Figure 4. Figure 4 shows that the morphology of the zeolite-X exhibit octahedral particle with a uniform particle shape. This indicates that the hydrothermal process at 100°C for 15 hours produced a homogeneous crystalline zeolite-X with a high degree of crystallinity.

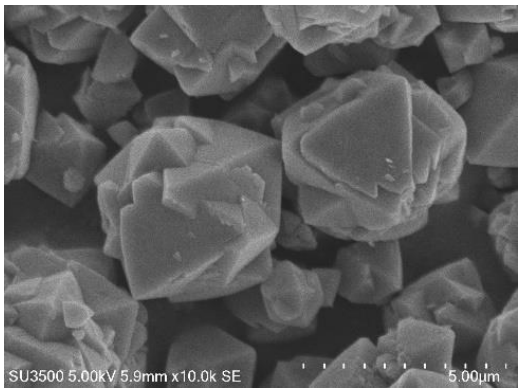

Figure 4. SEM Figure of Zeolite-X from bottom ash.

3.4. Hydrogen Adsorption

The hydrogen adsorption capacity of the zeolite-X was determined using the gravimetric method. The graph of the hydrogen adsorption capacity is shown in Figure5. Figure 5 shows that the hydrogen adsorption capacity of the zeolite-X increased continuously until 20 minutes, and then Levelled off and attained equibrium as the time was further increased. It might be due to the fact that initially there were abundant vacant adsorbent sites in the zeolite-X pore. With the progress of adsorption process, hydrogen gas adsorbed into the zeolite pore until completely reached equilibrium.
.

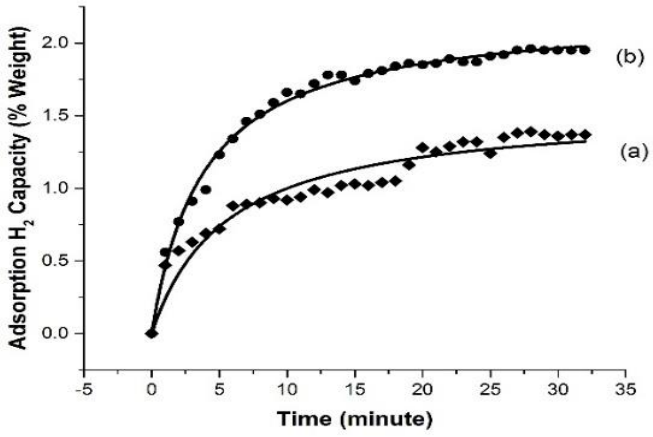

Figure 5. Graph of H_2 adsorption on (a) zeolite-X synthetic and (b) zeolite-X from bottom ash

Zeolite-X synthesized with pure chemicals has a lower value of adsorption capacity compared to the zeolite-X of the bottom ash which was about 1.03%wt of the capacity of the hydrogen gas. The zeolite-X of the bottom ash has an adsorption capacity of 1.60% wt. This value is greater 56% than zeolite-X from pure chemicals. The hydrogen storage capacity in the zeolite-X was 0.4% to 0.9 wt% under conditions of 30°C/100 bar [24-25]. This results indicate that the synthesized zeolite-X from bottom ash was more appropriate for hydrogen gas storage

Hydrogen gas adsorption process that occurs in zeolite-X belong to physisorption. Hydrogen gas physisorption process is highly dependent on the affinity of the gas on the surface of the adsorbent under certain conditions without the formation of chemical bonds. Adsorbents can absorb hydrogen gas easily to the surface of the material with weak interaction. In reciprocal interaction, asymmetric polarization of the electron charge is induced in the molecule that forms a temporary dipole moment and the hydrogen molecule becomes attracted by the electrostatic force. The interaction of the pull of the gas and the adsorbent comes from the force generated by changes in the charge distribution of the gas molecule and the surface of the adsorbent, thereby generating a pull between the induced and fluctuating dipole. However, at close distances the occurrence of overlap between the electron clouds of the gas molecules and the adsorbents results in repulsions that significantly increase rapidly [26].

FTIR instrument was used to study the interaction between hydrogen gas and the zeolite as shown in Figure 6.Figure 6 showed that the synthesized zeolite-X from the bottom ash have spesific character for zeolite-X. Spectra in 447 cm^{-1} region is a sign of bending vibration of TO_4. Double 6 ring structure connected with sodalite arrangement by absorbing band at 556 cm^{-1}. Vibration of symmetry from (Si-O-Al) at 666 cm^{-1}, while asymmetric strain vibration (Si-O-Al) at 949 cm^{-1}. In a previous study reported that the infrared spectra obtained on commercial zeolite-X occurred in regions 450 cm-1 to 1060 cm^{-1} with details of the region of 458 cm^{-1} is an indication of the bending vibration of TO, vibration symmetry in the area of 668-690 cm^{-1} and asymmetric vibrations occurred in the region 971-1060 cm^{-1}[27]. Other studies have also reported that zeolite-X has a characteristic functional group on the FTIR spectra at 456-1053 cm^{-1}. In addition to identify the typical character of zeolite-X, FTIR spectra results can also be used to determine the presence of solids such as zeolite-P and sodalite in the formed zeolite-X. Both impurities will block the double ring area on zeolite-X, thus the Infrared spectra for the double ring will not appear [28].

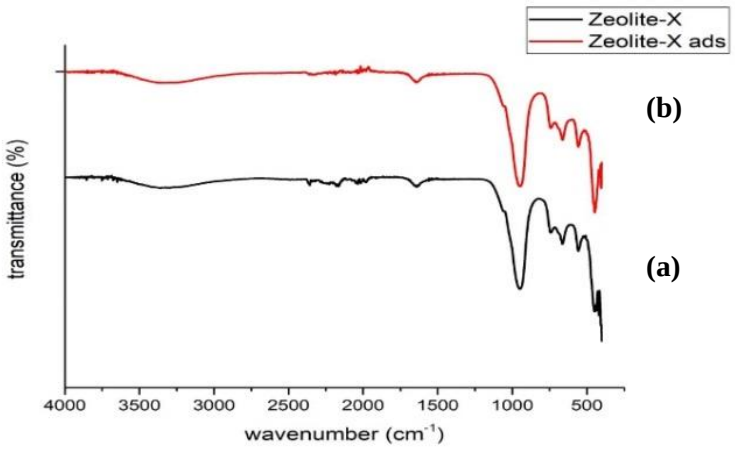

Figure 6. Spectra Zeolite-X before (a) adsorption, (b) after

The FTIR spectra of zeolite-X after the H_2 gas adsorption process in Fig. 6 (b) shows a difference with the zeolite-X initial spectra prior to adsorption. The difference is in the form of peak shift spectra and decrease in intensity. The peak in the 1640 cm^{-1} area decreased by 0.38%, while peak shift occurs for spectra at 3316 cm^{-1} to 3356 cm^{-1} along with low intensity decrease. The phenomenon of shifting and decreasing the intensity of the zeolite-X spectra results from the presence of a typical functional group interaction with the adsorbate used. FTIR spectra that experience a shift or decrease in intensity is the specific spectra for OH groups in H_2O molecules.

4. Conclusion

According to the discussion results, it can be concluded that high purity zeolite-X can be synthesized from the bottom ash through a fusion process with alkali at high temperatures, followed by

hydrothermal processes for 15 hours at 100°C. The result showed that zeolite-X synthesized from the bottom ash has hydrogen gas adsorption capacity greater than zeolite-X from pure chemicals, which is up to 1.60%.

5. References

[1] Hirscher M 2009 *Handbook of Hydrogen Storage: New Materials for Future Energy Storage* (Germany: Wiley-VCH Verlag GmbH and Co. KgaA) p 12

[2] Schlapbach L and Zuttel A 2001 Hydrogen- storage materials for mobile applications *J. Nature.* **414** p 353

[3] Zuttel A, Borgschulte A and Schlapbach L 2008 *Hydrogen as a Future Energy Carrier* (Germany: Willey – VCH)

[4] Strobel R., Garche J, Moseley P T, Jorissen L and Wolf G 2006 Hydrogen storage by carbon materials *J. Journal of Power Sources* **159** p 781

[5] Morris R E and Wheatley P S 2008 *Gas Storage in Nanoporous Materials* vol 47 (Germany: Wiley-VCH Verlag GmbH Co.) p 4966

[6] Breck W D 1974 *Zeolit Molecular Sieves* (New York: John Wiley & Sons, Inc.)

[7] Li J R, Ma Y, McCarthy M C, Sculley J, Yu J, Jeong H K, Balbuena P B, and Zhou H C 2011 Carbon dioxide capture-related gas adsorption and separation in metal-organic frameworks *J. Coordination Chemistry Reviews* **255** p 1791

[8] Hardie S M L, Garnett M H, Fallick A E, Rowland A P and Ostle N J 2005 Carbon Dioxide Capture Using a Zeolite Molecular Sieve Sampling System for Isotopic Studies (^{13}C and ^{14}C) of Respiration *J. Radiocarbon* **47** p 441

[9] Mosher K 2011 *The Impact of Pore Size on Methane and CO_2 Adsorption in Carbon* (Stanford: Stanford University)

[10] Chang H L and Shih W H 2000 Synthesis of Zeolite A and X from fly ash and Their Ion Exchange Behaviour With Cobalt Ion *J. Industrial Engineering Chemical Research* **39** p 4185

[11] Molina A and Poole C 2004 A Comparative Study Using Two Methods To Produce Zeolit from Fly Ash *J. Mineral Engineering* **17** p 167

[12] Miyake M, Kimura Y, Ohashi T, and Matsuda M 2008 Preparation Of Activated Carbon-Zeolite Composite Materials From Coal Fly Ash *J. Microporous and Mesoporous Materials* **112** p 170

[13] Kementerian Lingkungan Hidup 2006 *Pengelolaan Bahan dan Limbah Berbahaya dan Beracun* www.Lingkunganhidup.com.

[14] Yanti Y 2009 *Sintesis Zeolit A dan Zeolit Karbon Aktif dari Abu Dasar PLTU Paiton dengan Metode Peleburan : Thesis Magister* (Surabaya: Institut Teknologi Sepuluh Nopember)

[15] Zhely N H M 2012 *Sintesis Zeolit-X dari Abu Dasar Batubara dan Karakterisasinya sebagai Material Penyimpan Hidrogen : Prosiding Tugas Akhir* (Surabaya: Institut Teknologi Sepuluh Nopember)

[16] Robson H and Lillerud K P 2001 Verified Syntheses of Zeolitic Materials, second Revised Edition *J. Elsevier Science B. V.* p 150

[17] Faridah A M, Widiastuti N and Prasetyoko D 2012 *Karakterisasi Abu Dasar PLTU PAITON: Pengaruh Perlakukan Magnet, HCl, dan Fusi dengan NaOH : Prosiding Seminar Nasional Kimia Unesa* (Surabaya: Universitas Surabaya) p C198

[18] Wolf K J, Smeda A, Muller M, and Hilpert K 2005 Investigation on the in Fuence of Additives for SO2 Reduction during High Alkaline Biomass Combustion *J. Energy Fuels* **19** p 820

[19] Brady J E 1998 *Kimia Universitas, Asas dan Strukur Jilid I (Terjemahan Sukmariah, M. Kamianti, A., dan Tilda, S)* (Jakarta: Binarupa Aksara)

[20] Chang H and Shih W 2000 Synthesis of Zeolite A and X from fly ash and Their Ion Exchange Behaviour With Cobalt Ion *J. Industrial Engineering Chemical Research* **39** p 4185

[21] Chunfeng W, Jiansheng L, Xia S, Lianjua W, and Xiuyun S 2009 Evaluation of zeolites synthesized from fly ash as potential adsorbents for wastewater containing heavy metals *J.Enviro. Sci* **21** p 127

[22] Yaping Y, Xiaoqiang Z, Weilan Q, and Mingwen W 2008 Synthesis of Pure Zeolites from Supersaturated Silicon and Aluminium Alkali Extracts from Fused Coal Fly Ash *J. Fuel* **87** p 1880

[23] Handayani R F 2012 *Sintesis ZSM-5 Menggunakan Prekursor Zeolit Nano Kluster : Pengaruh Waktu Hidrotermal : Proseding Skripsi* (Surabaya : Departemen Kimia, Institut Teknologi Sepuluh Nopember)

[24] Lee H J, Kim Y M, Kweon O S and Kim I I 2007 Structural and morphological transformation of NaX zeolite crystals at high temperature *J. Journal of the European Ceramic Society* **27** p 561

[25] Walton K S, Abney M B and LeVan M D 2006 CO_2 adsorption in Y and X zeolites modified by alkali metal cation exchange *J. Microporous Mesoporous Mater* **91** p 78

[26] Saha B B, Jribi A, Koyama S and El-Sharkawi I I 2010 Carbon Dioxide Adsorption Isotherm on Activated Carbons *J. Journal of Chem.Eng* **56** p 1974

[27] Ozdemir D O 2013 Zeolite-X Synthesis with Different Sources *J. Journal of Chemical, Enviromental & Biological Sciences* **1** p 229

[28] Balkus J K and Ly T K 1991 The Preparation and Characterization of an X-Type Zeolite *J. Journal of Chemical Education* **68** p 1